

## ON THE LAMINAR COMBUSTION CHARACTERISTICS OF NATURAL GAS-SYNGAS-AIR MIXTURES

by

**Ning ZHANG<sup>a,b</sup>, Jie LIU<sup>a,b\*</sup>, Junle WANG<sup>a,b</sup>, and Hongbo ZHAO<sup>a,b</sup>**

<sup>a</sup> Department of Power Mechanical Engineering, Beijing Jiaotong University, Beijing, China

<sup>b</sup> Beijing Key Laboratory of New Energy Vehicle Powertrain Technology, Beijing, China

Original scientific paper

<https://doi.org/10.2298/TSCI171229255Z>

*In this study, the effects of hydrogen and CO addition on the laminar flame speed and flame instabilities of CH<sub>4</sub>/air mixture are investigated experimentally and numerically. Results show that laminar flame speeds increase almost linearly with the addition of hydrogen, which is mainly caused by the increase of the flame temperature and the thermal diffusivity of the mixture. However, it decreases with the increase of the pressure, which is mainly due to the increase of the mixture density and the enhancement of the termination reactions. The hydrodynamic instability is increased with the increase of hydrogen ratio and pressure, which is due to the reduction of the flame thickness. With the increase of hydrogen fractions and pressure, the Markstein lengths decrease obviously, which means the flame instability is enhanced. The addition of CO has little effect on the flame speeds and flame instabilities.*

Key words: syngas, laminar flame speed, flame instability

### Introduction

With the rapid development of the world economy and the increase of the global energy demand, air pollutants have become the major problems for the sustainable development of human society. Therefore, all countries in the world attach great importance on the clean alternative fuel researches. China is now in a period of rapid economic growth, and the environmental problems are particularly prominent. That is because coal is the main source of energy supply in China and the vast majority of coal is used to generate heat and power through direct burning, which produces great air pollutions. Therefore, exploiting and using of clean and high efficient coal combustion technology is imminent for China. The coal gasification technology, which is not only a clean combustion technology, but also a high efficient way for the utilization of coal resources, has a great potential for development. Coal gasification is the process of producing syngas, which is a mixture consisting primarily of CO, hydrogen (H<sub>2</sub>) and CH<sub>4</sub>, [1]. The synthetic gas was a popular alternative fuel in the gas turbine industry [2], and it can be used as fuel for the other internal combustion engines [3]. Due to the small lower heating value, synthesis gas can be blended with natural gas to achieve a higher thermal efficiency in combustion engines [4]. In addition, the natural gas has been recognized as the world's most practical alternative fuel [5]. The syngas composition can vary widely depending on the different types of raw materials and the methods of gasification process. Therefore, in

\* Corresponding author; e-mail: ljie@bjtu.edu.cn

order to design a flexible combustion system, it is necessary to investigate the fundamental combustion properties of the fuel mixture, such as flame instability and laminar flame speed, over a wide range of compositions.

Laminar flame velocity,  $S_{fl}$ , is one of the key fundamental parameters in combustion theory to reflect the combustion characteristics of the mixture. Moreover, it is an important parameter to confirm and develop the chemical reaction mechanisms. In particular, researchers investigated the effect of  $CO_2$  addition on the laminar burning velocity and flame stability of  $H_2$ -CO mixtures [6]. Other researchers studied the effect of nitrogen ( $N_2$ ) addition on the laminar flame speed of  $H_2/CO/O_2$  mixture [7]. The laminar flame speeds of  $H_2/CO$  mixtures at high pressures were investigated [8]. A detailed chemical kinetic mechanism for  $H_2$  and  $H_2/CO$  (syngas) mixtures had been updated [9]. In addition, laminar flame speeds, and mechanism validation for  $CH_4/H_2$  blends at elevated pressures were carried out [10]. Zhang *et al.* [11] studied the effects of  $H_2$  addition on the laminar flame speed of syngas by using three different kinetic mechanisms. The addition of  $H_2$  can increase the flame temperature and change the transport characteristics of the mixture, which enhance combustion intensity [12]. The addition of CO was directly involved in the chemical reaction through the elementary reaction  $OH + CO \leftrightarrow H + CO_2$ , which had a suppression effect on the combustion process [13]. Many research efforts have been devoted to the Lewis numbers, which has the important influence on the flames of the combustion [14]. Downstream interactions between lean pre-mixed flames with mutually different fuels of syngas and  $CH_4$  were numerically investigated [15]. More recently, the effect of  $CH_4$  addition on laminar flame speed and the cellular instabilities of syngas were investigated [16]. High multimode combustion instability was observed under certain particular compositions of  $H_2/CH_4$ /air mixture [17]. Most of these previous works deal with limited  $H_2$  and CO fractions in syngas composition. However, the laminar burning velocity of  $CH_4/H_2/CO$ /air mixture under wider range of  $H_2$  and CO fractions has not been sufficiently clarified.

From an academic point of view,  $H_2$  has much higher reactivity, lower density and higher diffusivity than any other hydrocarbons (HC), the addition of  $H_2$  will have an obvious effect on the flame propagation velocity and instability. Moreover, the chemical reaction characteristics and physical properties of CO are different with that of  $H_2$ . In addition, CO is the intermediate substances in the HC combustion process. Therefore, further analysis should be conducted to investigate the effect of  $H_2/CO$  addition on the combustion characteristics of  $CH_4$ /air mixture from the chemical and physical properties.

### **Experimental methodology and technique**

In this section, the experimental set-up, fuel/air mixture preparation process, data processing method, and the numerical method will be given.

#### *Experimental set-up*

The major components of the equipment include the mixture prepare system, constant volume combustion bomb, high speed Schlieren system, ignition system and the vacuum pumping system, as shown in fig. 1. The diameter and length of the cylindrical combustion chamber are 100 mm and 240 mm, respectively. The diameter and thickness of the two quartz windows installed on both sides of the vessel are 140 mm and 50 mm. The mixture was ignited by a couple of electrodes that are centrally located in the combustion vessel with the ignition energy of 80 mJ.

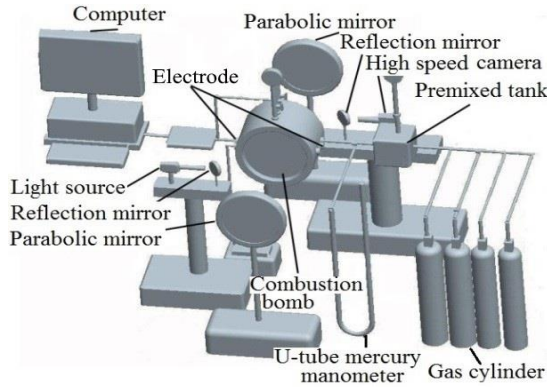


**Figure 1. Schematic representation of the experimental set-up**

The Red Lake MotionPro X4 Plus high speed digital camera was used to capture the flame propagation with the resolution of digital flame photographs setting as  $512 \times 512$  pixels at 5000 frames per second. Each flame diameter was determined with an accuracy of  $\pm 2$  pixel. The error of measured radius has its maximum value of 4% at small radius ( $r_u = 5$  mm) and the minimum value of 0.92% at large radius ( $r_u = 25$  mm). The combustion pressure was recorded by using the Kistler 6061B pressure transducer. The accuracy of pressure sensor is  $\pm 0.05$  bar. A type K thermocouple with an accuracy  $\pm 1$  K was

used to measure the initial temperature and the variation in initial temperature was  $298 \pm 2$  K. Thus, the relative error in initial temperature is 0.67%.

#### Fuel/air mixture preparation

In order to study the effects of syngas addition on the combustion characteristics of the natural gas/air mixtures, different  $H_2$  and CO mole fractions were used in the mixture. In this experiment,  $CH_4$  was used to represent natural gas, and  $H_2/CO$  mixture was used to represent syngas.

Moreover, in order to make the  $S_n-R_H$  plot appear as a linear relation in the subsequent data processing, the equivalence ratio and the  $H_2$  ratio were redefined as eqs. (1) and (2):

$$\phi_F = \frac{C_{CH_4} / (C_{CH_4} / C_A)_{st} + C_{CO} / (C_{CO} / C_A)_{st}}{C_A - C_{H_2} / (C_{H_2} / C_A)_{st}} \quad (1)$$

$$R_H = \frac{C_{H_2} + C_{H_2} / (C_{H_2} / C_A)_{st}}{C_{CH_4} + C_{CO} + [C_A - C_{H_2} / (C_{H_2} / C_A)_{st}]} \quad (2)$$

where  $C_i$  is the molar concentration of the  $i$  component, for example,  $(C_{CH_4}/C_A)_{st} = 0.105$ ,  $(C_{CO} + C_A)_{st} = 0.42$ ,  $(C_{H_2}/C_A)_{st} = 0.42$ .

In each experiment, the stoichiometric mixture is used. When preparing gas mixture, the molar concentration of CO and  $CH_4$  is first defined, and then the volume fractions of  $H_2$  and air can be obtained according to eqs. (1) and (2).

The mole fractions of CO in the fuel are defined as eq. (3):

$$X_{H_2} = \frac{C_{H_2}}{C_{H_2} + C_{CH_4}} \quad (3)$$

**Table 1. Fuel composition used in the experiments**

	Fuel composition		
	$R_H$	CO/(CO + CH <sub>4</sub> )	CH <sub>4</sub> /(CO + CH <sub>4</sub> )
0% CO	0.1-0.5	0	100
15% CO	0.1-0.5	15	75
30% CO	0.1-0.5	30	70
45% CO	0.1-0.5	45	55

The fuel composition used in the experiments and calculations can be found in tab. 1.

The normalized sensitivity coefficient with respect to the laminar flame speed can be calculated with eq.

(4), which provides quantitative understanding how the flame speed depends on the chemical kinetics in the model:

$$F_{\text{sen,R}} = \frac{A_i}{X} \frac{\partial X}{\partial A_i} \quad (4)$$

where  $A_i$  is the  $A$ -factors of the reaction rate coefficients, and  $X$  is the flame speed.

#### Data processing method

For the spherical propagate flame, the stretched flame velocity,  $S_n$ , which reflects the flame propagation speed relative to the chamber wall, is derived from the flame radius versus time [18], which can be calculated by eq. (5):

$$S_n = \frac{dr_u}{dt} \quad (5)$$

where  $r_u$  is the radius of the flame measured from the Schlieren photograph and  $t$  is the time after the ignition. The flame stretch rate, representing the expanding rate of flame front area, can be simplified as eq. (6):

$$\alpha = \frac{d(\ln A)}{dt} = \frac{2}{r_u} \frac{dr_u}{dt} = \frac{2}{r_u} S_n \quad (6)$$

In the early stage of flame expansion, where cylinder pressure has little changes, there is a linear relationship between the stretched flame speed and the flame stretch rate, that is in the form of eq. (7):

$$S_1 - S_n = L_b \alpha \quad (7)$$

where  $L_b$  is the Markstein length of the burned gas. The simple relationship links the unstretched burning velocity to the unstretched laminar flame speed was eq. (8):

$$u_1 = \frac{\rho_b}{\rho_u} S_1 \quad (8)$$

where  $\rho_b/\rho_u$  is the density ratio,  $\rho_b$  and  $\rho_u$  are the densities of the burned and unburned gases, separately.

#### Numerical method

The PREMIX code was employed to calculate the speed of the freely propagating premixed laminar flame [19]. In addition, the CHEMKIN II [20] and TRANSPORT [21] subroutine libraries were integrated in the code. Moreover, the multi-component diffusion coefficients, thermal conductivities and thermal diffusion were used in the transport model. The convective terms and the diffusive terms were calculated by windward difference and central difference, respectively. The unburned mixture temperature was set as 298 K with the pressures of 1 bar and 3 bar. The solution was obtained with the curvature and gradient values of 0.025 and the grid points were over than 500. The beginning and end of the computational boundary were set as  $x = -2.0$  cm and  $x = 10.0$  cm, respectively.

Generally, GRI-mech 3.0 mechanism was used to simulate the combustion of  $\text{CH}_4$ /air mixture. When the fuel is changed from single fuel to triple fuels mixture, the predicted flame speeds of  $\text{CH}_4/\text{H}_2/\text{CO}$  air mixtures were consistent with the experimental data at lean to stoichiometric conditions. However, the deviations were more obvious at rich flames [22]. Therefore, a modification of the reaction rates of the key reactions in the GRI-mech 3.0

mechanism is needed to improve the flame speed prediction. So, in the following discussion, the new modified GRI-mech 3.0 model with 11 updated reaction rates will be employed, which can be found in our previous research [23].

### Results and discussion

In order to investigate the effects of H<sub>2</sub> and CO addition on the characteristics of the CH<sub>4</sub> laminar flame, the flame speeds of CH<sub>4</sub>/H<sub>2</sub>/CO air mixtures with X<sub>CO</sub> from 0 to 0.45 and R<sub>H</sub> from 0.10 to 0.50 were investigated in this study under the pressures of 1 bar and 3 bar.

Figures 2 and 3 show the experimental and calculation laminar flame speeds with various H<sub>2</sub> and CO mole fractions under pressures of 1 bar and 3 bar. Although there are some difference between the experimental results and the predicted ones, the trends of the measured and computed laminar flame speeds showed good agreement. In addition, the results indicate that the calculated laminar flame speeds increase almost linearly with the increase of R<sub>H</sub>. However, a noticeable bending is shown in the experimental result, which is also found by other researchers [24]. Figures 2 and 3 also show that as the initial pressure increases, the flame speed decreases, which is mainly due to the increase of the mixture density.

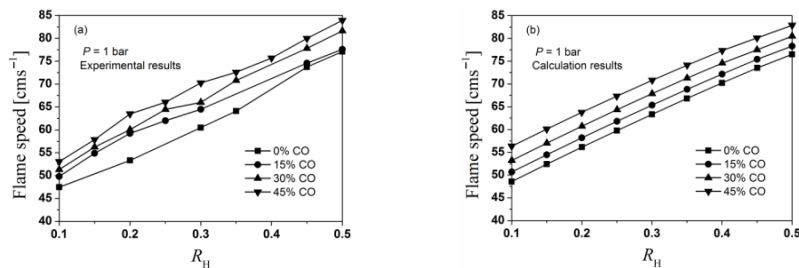


Figure 2. Experimental and theoretical values of the flame speed under 1 bar

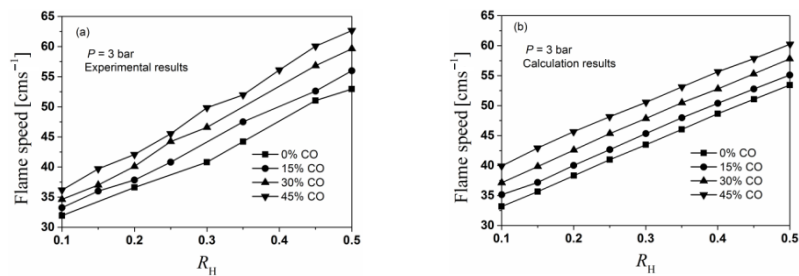
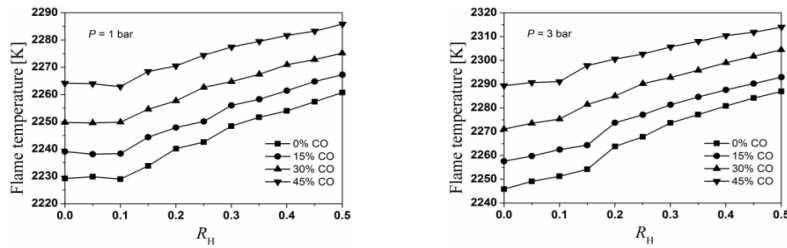


Figure 3. Experimental and theoretical values of the flame speed under 3 bar

According to the classic combustion theory, the flame temperature and the thermal diffusivity have significant effect on the laminar flame speed. Therefore, the flame temperature and the thermal diffusivity with different H<sub>2</sub> and CO mole fractions are provided in figs. 4 and 5. The flame temperatures of the mixture increase with the addition of both H<sub>2</sub> and CO mole fractions. The tendency is almost the same as the flame speed vs. H<sub>2</sub> and CO fractions. The thermal diffusivity increases obviously with the addition of H<sub>2</sub>. However, the addition of CO has almost no effect on the thermal diffusivity. Therefore, the addition of H<sub>2</sub> will increase both the flame temperature and the thermal diffusivity of the mixture, which will promote the flame speed. The dominant effect of CO addition on the flame speed is through the thermal

aspect. Furthermore, the flame temperature increases with the increase of pressure, while the thermal diffusivity decreases when pressure increase.



**Figure 4. Calculated flame temperatures under different CO and H<sub>2</sub> mole fractions**

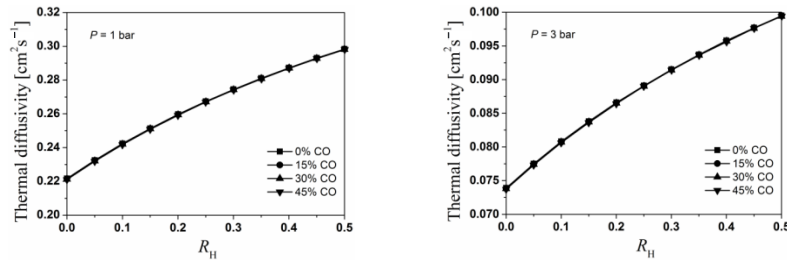


**Figure 5. Calculated thermal diffusivity under different CO and H<sub>2</sub> mole fractions**

The 20 elementary reactions exhibiting the largest normalized sensitivity coefficient with respect to the laminar flame speed are shown in fig. 6, where fig. 6(a) is at 1 bar and fig. 6(b) is at 3 bar. The main chain branching/propagating elementary reactions are  $\text{H} + \text{O}_2 \rightleftharpoons \text{O} + \text{OH}$ ,  $\text{OH} + \text{CO} \rightleftharpoons \text{H} + \text{CO}_2$ ,  $\text{OH} + \text{H}_2 \rightleftharpoons \text{H} + \text{HO}_2$ , and  $\text{H} + \text{HO}_2 \rightleftharpoons 2\text{OH}$ . In addition, the major chain termination reactions are  $\text{H} + \text{CH}_3 + \text{M} \rightleftharpoons \text{CH}_4 + \text{M}$  and  $\text{H} + \text{O}_2 + \text{M} \rightleftharpoons \text{HO}_2 + \text{M}$ . The chain branching/propagating reactions produce H, O and OH radicals, which will promote the combustion process and increase the flame speed. However, the chain termination reactions will reduce the radical concentrations and suppress the oxidation process, which will reduce the flame speed. Furthermore, the branching/propagating reactions are two-body reactions, which are temperature-sensitive reactions. While the termination reactions are three-body reactions and they are temperature insensitive. Thereby the branching and termination reactions can be enhanced relative to each other by increasing the adiabatic flame temperature and system pressure, respectively [25]. This is the other reason for the flame speed reduction under high-pressure conditions.

There are three main mechanisms influencing the flame stability of the laminar flame, namely, the hydrodynamic factor, the diffusional thermal factor and the buoyancy-driven factor. Where the hydrodynamic instability, also called as the Landau-Darrieus instability, is caused by the density jump across the flame. The changing of the flow velocity due to the thermal expansion makes the local velocities of the approach flow and the flame speed no longer balance each other. Since all combustion processes are accompanied by thermal expansion, the hydrodynamic instability is always present. Nevertheless, this factor only appeared when the flame propagates to a certain condition. Such as the flame radius is large eno-

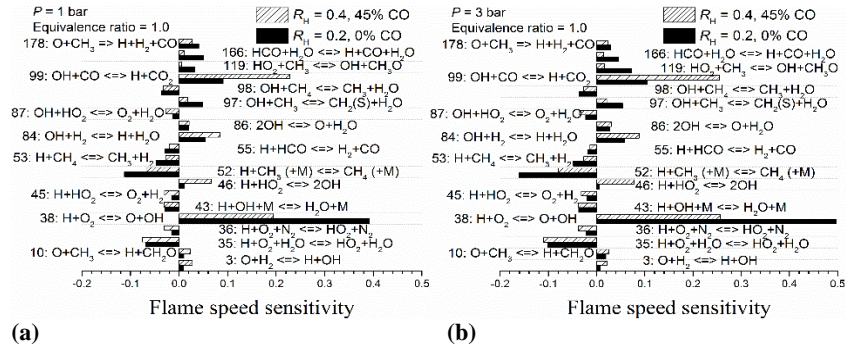


**Figure 6. Normalized logarithmic sensitivity coefficients of the laminar flame speed**

ugh to have an effect on the flame propagation stability. The diffusional thermal instability is caused by the preferential diffusion of the mass near the flame front face relative to the heat, which is mainly determined by the premixed gas of the reaction components. A flame is diffusively stable if it is abundant in the more mobile reactant. The buoyancy-driven instability occurs in the flame front when negative density stratification has appeared in the same direction as the body force. It is only occurring when the flame propagation rate is very slow, such as near the combustion limit.

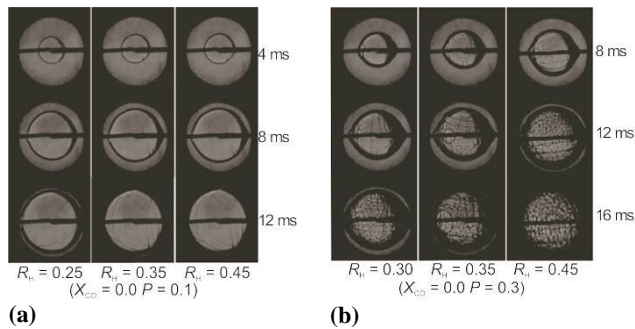


**Figure 7. Schlieren photographs of CH<sub>4</sub>-syngas-air flames with different  $R_H$**

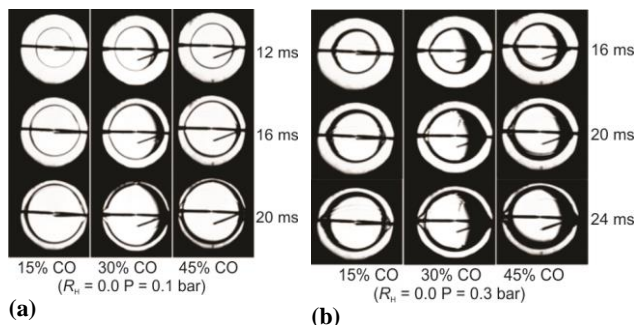


**Figure 8. Schlieren photographs of CH<sub>4</sub>-syngas-air flames with different CO mole fractions**

Figures 7(a) and 7(b) compare the cellular instabilities in CH<sub>4</sub>-syngas-air flames at the same  $X_{CO}$  dilution ratio under different pressures. As shown in figs. 7(a) and 7(b), at low pressure conditions, no flame instabilities have appeared with different H<sub>2</sub> mole fractions. However, at high pressure conditions, flame instabilities have appeared with the same H<sub>2</sub> mole fractions as the low pressure conditions. Moreover, with the increase of H<sub>2</sub> fraction, the cellular flame structure is enhanced and more cracks appear in the flame surface. These cracks will be transformed into the un-stable cellular structure, which will accelerate the flame speed. However, there are no flame instabilities at low to high pressure conditions with the increase of CO mole fractions, as shown in figs. 8(a) and 8(b). This means that the addition of CO has little effect on the flame instabilities of the CH<sub>4</sub>-

syngas-air flames. During the flame speed extraction process, the flames with radiuses less than 25 mm were used to minimize the effect of the cracks on the flame speeds.

The hydrodynamic instability is enhanced with the decrease of flame thickness and an increase of density ratio. Therefore, the calculated flame thicknesses under different  $H_2$  and CO mole fractions and pressure conditions are shown in figs. 9(a) and 9(b). It is shown that the flame thickness decrease slightly with the increase of  $H_2$  fraction. The pressure increase has a much remarkable effect on the reduction of flame thickness, which will significantly promote the hydrodynamic instability [26]. In addition, the addition of CO has less influence on the reduction of flame thickness compared with the addition of  $H_2$ , which means it has little effect on the flame instability. Moreover, fig. 9 shows that the density ratio increases slightly with the increase of  $H_2$  and CO fractions, which reduces the hydrodynamic instability. However, the density ratio reduces slightly with the increase of the pressure, which promotes the hydrodynamic instability. This indicates that the main reason for the increase the instability of the combustion with the increase of the initial pressure is the reduction of the flame thickness.

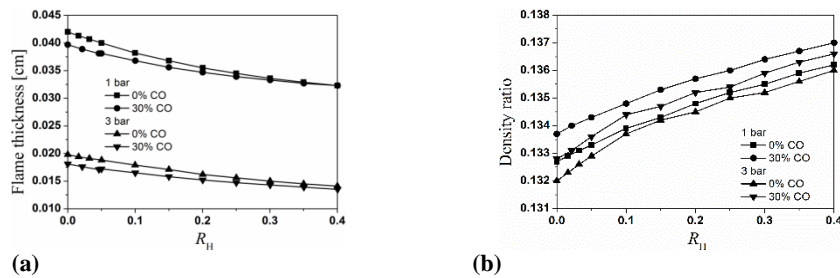


Figure 9. Theoretical flame thickness and density ratio under different pressures

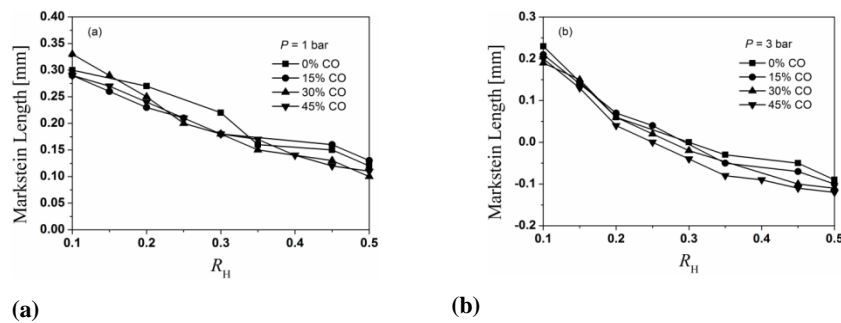


Figure 10. Markstein lengths of the premixed flames under different pressures

The Markstein length represents the effect of the flame speed on the flame stretch rate. For a negative Markstein length flame, the flame speed increase with the increase of the stretch rate. Any protuberance occurs on the flame front will enhance the flame instability [22]. Figure 10 plots the measured Markstein lengths of the premixed flames as a function of  $R_H$  at the initial pressures of 1.0 and 3.0 bars. With the increase of  $H_2$  fractions, the Markstein lengths decrease obviously. In addition, the Markstein lengths become negative when the  $R_H$  larger than 0.3 under the pressure of 3 bar, which means the flame instability is enhanced. The Markstein lengths of the flame decrease slightly with the addition of CO, and it decreases obviously with the increase of pressure.

## Conclusions

In this study, the effects of H<sub>2</sub> and CO addition on the laminar flame speed and flame instabilities of CH<sub>4</sub>/air mixture were investigated experimentally and numerically at room temperature under different pressures. The results obtained are summarized as follows.

- Comparisons of the predicted flame speed with the measured data indicate that the trends of the measured and computed laminar flame speeds showed good agreement. In addition, the results indicate that the calculated laminar flame speeds increase almost linearly with the increase of  $R_H$ . However, a noticeable bending is shown in the experimental result.
- The flame temperatures of the mixture increase with the addition of both H<sub>2</sub> and CO mole fractions. The thermal diffusivity increases obviously with the addition of H<sub>2</sub>. However, the addition of CO has almost no effect on the thermal diffusivity. Furthermore, the flame temperature increases with the increase of pressure, while the thermal diffusivity decreases when pressure increase.
- Sensitivity analysis was performed to identify the dominant reactions with respect to the laminar flame speed. It is found that the branching and termination reactions can be enhanced relative to each other by increasing the adiabatic flame temperature and system pressure, which is the other reason for the flame speed reduction under high pressure conditions.
- At low pressure conditions, no flame instabilities appeared with different H<sub>2</sub> mole fractions. However, at high pressure conditions, flame instabilities have appeared with the same H<sub>2</sub> mole fractions as the low pressure conditions. Moreover, with the increase of H<sub>2</sub> fraction, the cellular flame structure is enhanced. However, no flame instabilities appeared at low to high pressure conditions with the increase of CO mole fractions.
- The flame thickness and Markstein length decrease with the increase of H<sub>2</sub> fraction; the pressure increase has a much more remarkable effect on the reduction of flame thickness and Markstein length, which will significantly promote the hydrodynamic instability. The addition of CO has little effect on the flame instabilities of the CH<sub>4</sub>-syngas-air flames.

## Acknowledgment

This work was supported by *the Fundamental Research Funds for the Central Universities*.

## Nomenclature

$A$	– flame area, [m <sup>2</sup> ]	$u_l$	– unstretched laminar burning velocity, [ms <sup>-1</sup> ]
$A_i$	– $A$ -factors of the reaction rate coefficients	$X$	– flame speed
$C_i$	– molar concentration of the $i$ component	<i>Greek symbols</i>	
$L_b$	– Markstein length of burned gases	$\alpha$	– flame stretch rate, [s <sup>-1</sup> ]
$R_H$	– H <sub>2</sub> ratio	$\phi_F$	– equivalence ratio
$r_u$	– radius of the flame, [mm]	$\rho_b$	– density of burned gases, [kgm <sup>-3</sup> ]
$t$	– time, [s]	$\rho_u$	– density of unburned gases, [kgm <sup>-3</sup> ]
$S_l$	– unstretched flame speed, [ms <sup>-1</sup> ]		
$S_n$	– stretched flame speed, [ms <sup>-1</sup> ]		

## References

- [1] Cvetković, S. M., *et al.*, Electricity Production from Biogas in Serbia Assessment of Emissions Reduction, *Thermal Science*, 20 (2016), 4, pp. 1333-1344
- [2] Kjarstad, J., Johnsson, F., The Role of Biomass to Replace Fossil Fuels in a Regional Energy System – The Case of West Sweden, *Thermal Science*, 20 (2016), 4, pp. 1023-1036

- [3] Boehman, A. L., Corre, O. L., Combustion of Syngas in Internal Combustion Engines, *Combustion Science & Technology*, 180 (2008), 6, pp. 1193-1206
- [4] Hagosa, F. Y., *et al.*, Methane Enrichment of Syngas (H<sub>2</sub>/CO) in a Spark-Ignition Direct-Injection Engine: Combustion, Performance and Emissions Comparison with Syngas and Compressed Natural Gas, *Energy*, 90 (2015), Part 2, pp. 2006-2015
- [5] Papagiannakis, R. G., *et al.*, Emission Characteristics of High Speed, Dual Fuel, Compression Ignition Engine Operating in a Wide Range of Natural Gas/Diesel Fuel Proportions, *Fuel*, 89 (2010), 7, pp. 1397-1406
- [6] Prathap, C., *et al.*, Effects of Dilution with Carbon Dioxide on the Laminar Burning Velocity and Flame Stability of H<sub>2</sub>-CO Mixtures at Atmospheric Condition, *Combustion & Flame*, 159 (2012), 2, pp. 482-492
- [7] Burke, M. P., *et al.*, Negative Pressure Dependence of Mass Burning Rates of H<sub>2</sub>/CO/O<sub>2</sub> /Diluent Flames at Low Flame Temperatures, *Combustion & Flame*, 157 (2010), 4, pp. 618-631
- [8] Sung, C. J., Law, C. K., Fundamental Combustion Properties of H<sub>2</sub>/CO Mixtures: Ignition and Flame Propagation at Elevated Pressures, *Combustion Science & Technology*, 180 (2008), 6, pp. 1097-1116
- [9] Keromnes, A., *et al.*, An Experimental and Detailed Chemical Kinetic Modeling Study of Hydrogen and Syngas Mixture Oxidation at Elevated Pressures, *Combustion & Flame*, 160 (2013), 6, pp. 995-1011
- [10] Donohoe, N., *et al.*, Ignition Delay Times, Laminar Flame Speeds, and Mechanism Validation for Natural Gas/Hydrogen Blends at Elevated Pressures, *Combustion & Flame*, 161 (2014), 6, pp. 1432-1443
- [11] Zhang, Y., *et al.*, Laminar Flame Speed Studies of Lean Premixed H<sub>2</sub>/CO/Air Flames, *Combustion & Flame*, 161 (2014), 10, pp. 2492-2495
- [12] Joo, S., *et al.*, NO<sub>x</sub> Emissions Characteristics of the Partially Premixed Combustion of H<sub>2</sub>/CO/CH<sub>4</sub> Syngas Using Artificial Neural Networks, *Applied Thermal Engineering*, 80 (2015), Apr., pp. 436-444
- [13] Wu, C. Y., *et al.*, Effects of CO Addition on the Characteristics of Laminar Premixed CH<sub>4</sub>/Air Opposed-jet Flames, *Combustion and Flame*, 156 (2009), 2, pp. 362-373
- [14] Kim, T. H., *et al.*, Effects of Preferential Diffusion on Downstream Interaction in Premixed H<sub>2</sub>/CO Syngas-air Flames, *International Journal of Hydrogen Energy*, 37 (2012), 16, pp. 12015-12027
- [15] Kim, J. S., *et al.*, A Study on Flame Structure and Extinction in Downstream Interaction between Lean Premixed CH<sub>4</sub>-Air and (50% H<sub>2</sub> + 50% CO) Syngas-Air Flames, *International Journal of Hydrogen Energy*, 36 (2011), 9, pp. 5717-5728
- [16] Lapalme, D., Seers, P., Influence of CO<sub>2</sub>, CH<sub>4</sub>, and Initial Temperature on H<sub>2</sub>/CO Laminar Flame Speed, *International Journal of Hydrogen Energy*, 39 (2014), 7, pp. 3477-3486
- [17] Hermanns, R., Laminar Burning Velocities of Methane-Hydrogen-Air Mixtures, *Journal of Loss Prevention in the Process Industries*, 24 (2007), Jan., pp. 648-655
- [18] Beeckmann, J., *et al.*, Experimental and Numerical Investigation of Iso-Octane, Methanol and Ethanol Regarding Laminar Burning Velocity at Elevated Pressure and Temperature, SAE technical paper, 2009-01-1774, 2009
- [19] Kee, R. J., *et al.*, Premix: A Fortran Program for Modelling Steady Laminar One Dimensional Premixed Flames, Report No. SAND85-8240, Sandia National Laboratories, Livermore, Cal., USA, 1985
- [20] Kee, R. J., *et al.*, CHEMKIN-II: A FORTRAN Chemical Kinetics Package for the Analysis of Gas-phase Chemical Kinetics, Report No. SAND96-8216, Sandia National Laboratories, Livermore, Cal., USA, 1986
- [21] Kee, R. J., *et al.*, A FORTRAN Computer Code Package for the Evaluation of Gas-phase Viscosities, Conductivities, and Diffusion Coefficients, Report No. SAND83-8209, Sandia National Laboratories, Livermore, Cal., USA, 1983
- [22] Vu, T. M., *et al.*, Measurements of Propagation Speeds and Flame Instabilities in Biomass Derived Gas-air Premixed Flames, *International Journal of Hydrogen Energy*, 36 (2011), 18, pp. 12058-12067
- [23] Liu, J., *et al.*, Numerical Study of the Chemical, Thermal and Diffusion Effects of H<sub>2</sub> and CO Addition on the Laminar Flame Speeds of Methane-Air Mixture, *International Journal of Hydrogen Energy*, 40 (2015), 26, pp. 8475-8483
- [24] Cheng, T. S., *et al.*, An Experimental and Numerical Study on Characteristics of Laminar Premixed H<sub>2</sub>/CO/CH<sub>4</sub>/air Flames, *International Journal of Hydrogen Energy*, 36 (2011), 20, pp. 13207-13217
- [25] Egolfopoulos, F. N., Law, C. K., Chain Mechanisms in the Overall Reaction Orders in Laminar Flame Propagation, *Combustion and Flame*, 80 (1990), 1, pp. 7-16
- [26] Landau, L., On the Theory of Slow Combustion, *Acta Physicochim URSS*, 19 (1944), Jan., pp. 77-88